Transactions, **SMiRT-26**
Berlin/Potsdam, Germany, July 10-15, 2022
Division IV

MODELING OF VERTICAL COMPONENT GROUND MOTION FOR SOIL-STRUCTURE-INTERACTION ANALYSES

Norman Abrahamson[1], Camilo Pinilla-Ramos[2], Payman Tehrani[3], Michael Perez[4], Alex Krimotat[5]

[1] Consultant, SC Solutions, Sunnyvale, USA (nabrahamson@scsolutions.com)
[2] Graduate Student, University of California, Berkeley, CA, USA (camilo.pinilla@berkeley.edu)
[3] Principal Engineer, SC Solutions, Sunnyvale, USA (ptehrani@scsolutions.com)
[4] Senior Engineer, SC Solutions, Sunnyvale, USA (mperez@scsolutions.com)
[5] Vice president, SC Solutions, Sunnyvale, USA (alex@scsolutions.com)

ABSTRACT

The standard assumption of modelling the vertical component by vertically propagating P waves underestimates the spatial variability of the vertical ground motion over the dimension of the foundation of large structures, which can lead to very large vertical floor spectra at high frequencies. Modelling the vertical ground motion as inclined P-SV waves and including stochastic variability to the velocity structure for the Soil-Structure Interaction (SSI) analysis adds complexity to the vertical wave field, but it is not enough to match the complexity in observed vertical ground motions as measured by the spatial coherency from dense seismic arrays. The coherency between two stations is controlled by the standard deviation of the phase differences between the seismograms at the two stations. The complexity in the input motions can be increased by adding separation-distance-dependent and frequency-dependent variability of the phase angles to the phase of the input motions so that the empirical coherency is recovered. The additional phase variability is added to the seismogram over multiple short time windows to maintain the nonstationary characteristics of the input motion. This allows the physics-based P-SV wave propagation to be combined with empirical adjustments on the input motion to both preserves the deterministic wave propagation features of the SSI as well as being consistent with the empirical coherency models for the vertical component. The result is greater spatial variability in the motions at the foundation of the structure which should reduce the overestimation of the vertical floor spectra at high frequencies.

INTRODUCTION

In typical SSI analyses, the wave propagation is simplified: the horizontal component is modelled as vertically propagating SH waves and the vertical component is modelled as vertically propagating P waves. This simplification typically leads to reasonable results for the horizontal component, but not for the vertical component. Strong-motion data recorded at distances less than 30 km show that the peak motion on the vertical component occurs during the S-wave window about 70% of the time indicating that peak amplitudes of vertical ground motions contain significant SV waves which cannot be adequately represented by vertically propagating P waves. The assumption that the vertical component is only vertically propagating P waves that are coherent spatially can lead to very large vertical components in structures. A different approach is needed to have a realistic representation of the wave propagation for the vertical component of ground motion.

The spatial coherency of the vertical component can be used as a measure of the effects of the complex wave propagation (mixture of P and SV waves) that makes up the vertical component of the ground motion. We use data from dense seismic arrays described in EPRI (2007) to evaluate the complex wavefield for the vertical ground motions. The vertical coherency from recorded earthquakes is compared to the vertical coherency from numerical simulations in a stochastic medium with inclined P-SV waves for a block with a dimension of 1 km on a side. The vertical-component coherency from the numerical simulations overestimates the observed coherency, indicating that more complexity in the input motions to the SSI is needed. In this paper, we develop a method to add the appropriate additional complexity to the input motions, such that when combined with the physical modelling of the P-SV waves in a stochastic medium, the resulting vertical-component coherency is consistent with the coherency from dense array recordings of earthquakes.

COHERENCY FROM SIMULATIONS USING STOCHASTIC VELOCITY STRUCTURE

One approach to SSI analysis that includes spatial variability of the ground motion is to use numerical simulations with a stochastic velocity structure; however, such simulations do not capture the frequency and separation distance scaling seen in empirical data. One example of such numerical simulation is to study the coherency of the vertical component using the program SW4 (Petersson and Sjogreen, 2015, 2018) with a stochastic velocity structure. The simulations were conducted for a range of variances and correlation lengths. An example of the variability in the velocity structure are shown in Figure 1, and the resulting coherency of the vertical component for a separation distance of 100 m is shown in Figure 2. The tanh transformation of the coherency is used so that the coherency is approximately normally distributed. For comparison, the coherency for the horizontal and vertical components from 9 earthquakes recorded by the Chiba, Japan array are shown in Figures 3 and 4 for separation distances of 20 m and 100 m. The empirical data shows that the coherency on the vertical component decays more rapidly with distance than with frequency. That is, a factor of 5 change in the frequency from 1 to 5 Hz for 20 m separation changes the coherency much less than a factor of 5 change in the separation distance from 20 m to 100 m. This is in contrast to the scaling of the coherency for the horizontal component which has a weaker decay with separation distance that the vertical component as shown in Figure 3. Similar results were found using the RealESSI simulation program (Jeremic et al, 2021). This indicates that the wave propagation for the vertical component is much more complex than for the horizontal component.

The frequency dependence of the vertical-component coherency from the simulations shown in Figure 2 has the same general shape as the empirical data, but it does not decay as fast at 100 m as the empirical data. Even using large variances of the velocity structure, the vertical-component coherency from the simulations does not decay as fast with frequency as observed from the earthquake data. Zerva (2009) shows results from simple models of the coherency for a stochastic layer that also shows that the coherency is overestimated at high frequencies. We conclude that a stochastic velocity structure with the P-SV waves captures some but not all of the complexity in the vertical component ground motion. Greater complexity in the input motions into the site velocity structure is needed to match the observed frequency dependence of the empirical coherency for the vertical component. The following section provides a method for adding complexity to the input motion to match a target vertical coherency function.

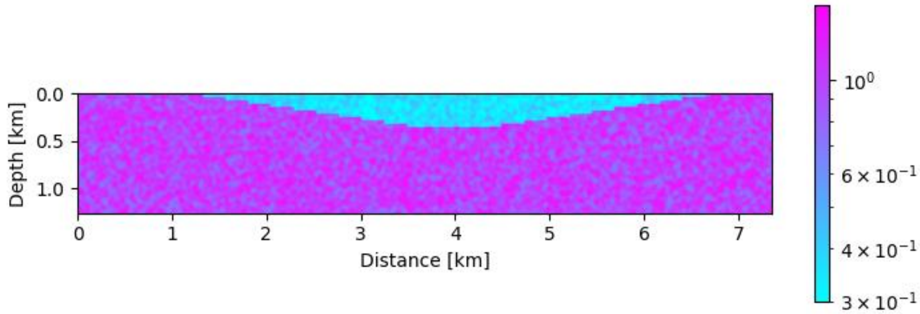

Figure 1. Example of the stochastic variations about a velocity structure with a sedimentary basin. The shear-wave velocity is shown in km/s.

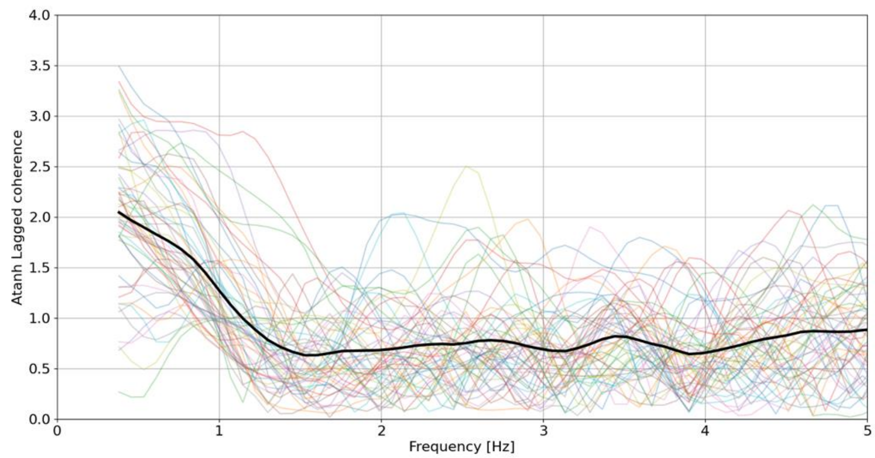

Figure 2. Example of the coherency of the vertical component for 100m separation for the stochastic velocity profile shown in Figure 1. The source is input on the lower left-hand side to represent an inclined wave. The simulations are valid up to 5 Hz.

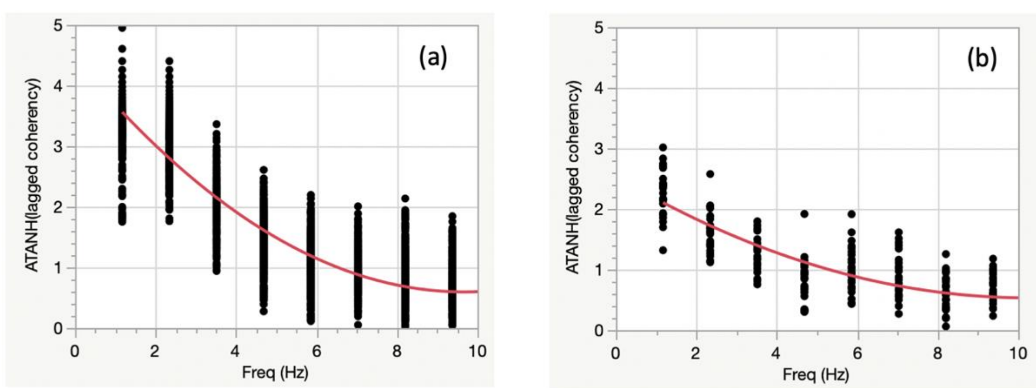

Figure 3. Frequency dependence of the empirical coherency for the horizontal component from 9 earthquakes recorded by the Chiba array. (a) 20 m separation. (b) 100 m separation

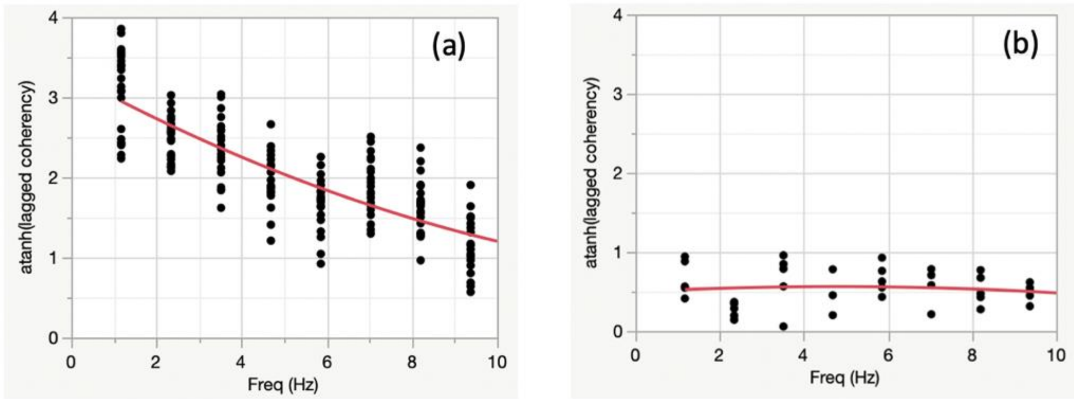

Figure 4. Frequency dependence of the empirical coherency for the vertical component from 9 earthquakes recorded by the Chiba array. (a) 20 m separation. (b) 100 m separation

COHERENCY AND THE STANDARD DEVIATION OF THE PHASE DIFFERENCE

The lagged coherency between the ground motion at station *k* and *l* is given by:

$$\gamma_{kl}(f) = \frac{|\bar{S}_{kl}(f)|}{\sqrt{\bar{S}_{kk}(f)\,\bar{S}_{ll}(f)}} \tag{1}$$

in which $\bar{S}_{kl}(f)$ is the smoothed cross spectrum given by:

$$\bar{S}_{kl}(f_i) = \sum_{j=-n}^{n} w_j\, \bar{S}_{kl}(f_{i+j}) \tag{2}$$

and w_j is a frequency window. Because coherency is normalized by the amplitude, the coherency mainly depends on the variability of phase of the cross spectrum over the frequency window and not on the amplitude spectrum.

The variability of the phase of the cross spectrum can be parameterized by the standard deviation of the phase. With the phase being restricted to [-π,π], phases of -π and π are the same but a simple computation of the standard deviation would treat those as being very different. To have a meaningful standard deviation, the standard deviation is computed for a range of phase shifts, and the minimum standard deviation is found. An example of this process is shown in Figure 5.

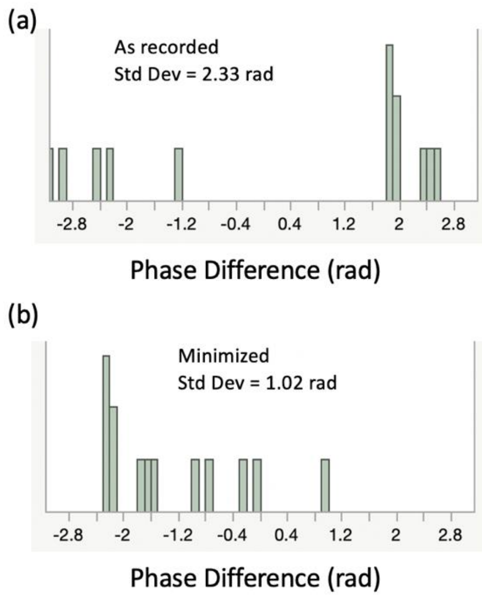

Figure 5. Example of measuring the standard deviation of the phase differences. (a) as recorded, the phase difference warp around. (b) shifted phase difference to minimize the standard deviation.

For both empirical earthquake data and numerical simulations in a stochastic medium, the coherency scales with the standard deviation of the phase. The relations of the coherency and the standard deviation of the phase from earthquake data and SW4 simulations are shown in Figure 6. The correlation is similar for both the empirical and simulated data sets indicating that the standard deviation of the phase difference is a good proxy for the coherency.

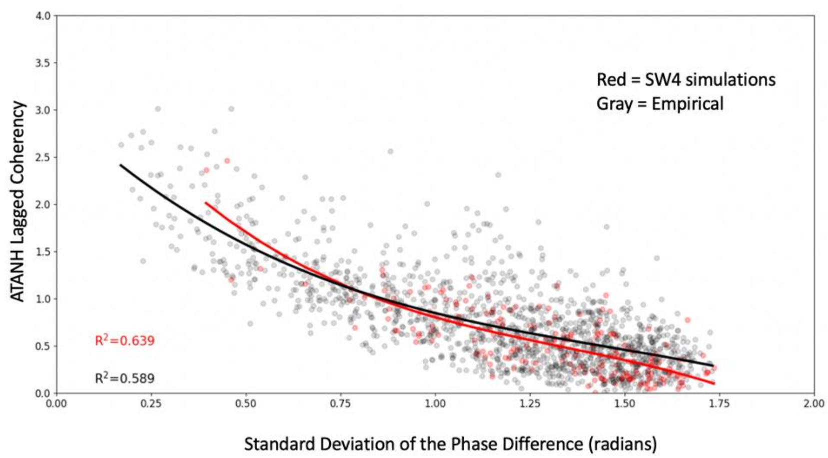

Figure 6. Correlation of the coherency with the standard deviation of the phase difference.

ADDING COMPLEXITY TO THE INPUT MOTIONS

The relation between the coherency and the standard deviation of the phase difference provides a simple method to modify the SW4 simulations to reduce the coherency to match a target empirical coherency model. The desired coherency can be related to a total standard deviation of the phase difference. The difference between the desired variance of the phase difference and the variance from the simulations provides the amount of variance of the phase difference to be added to the simulations as shown in equation (2).

$$\sigma_{\Delta\phi_{add}} = \sqrt{\sigma^2_{\Delta\phi,Target} - \sigma^2_{\Delta\phi,SIM}} \tag{2}$$

This method can only be used to add complexity (reduce the coherency) to the input motions obtained from SW4 simulations at the boundaries of the SSI model. We assume that the reduced domain method (e.g. Bielak et al, 2001) is used to perform SSI analysis.

Given the variability of the phase angles to be added to the input motion for each frequency and separation distances, a 2-D variogram of $\Delta\phi_{add}$ as a function of the separation distance on a horizontal plane is constructed for each frequency. Random samples of the phase differences that are compatible with the variogram are generated using a standard Cholesky decomposition. The generated phase differences are added to the input motion along the bottom of the reduced SSI analysis domain (e.g. Bielak et al, 2001). For the input motions along the sides of the SSI analysis domain, the phase difference from the point directly below is used. That is, there is no additional variability added in the vertical direction. This approach is based on observations that the coherency in the vertical separation direction is mainly controlled by the deterministic wave propagation effects that are already captured by the wave propagation in SW4.

CONSTRAINTS ON THE NON-STATIONARITY OF THE TIME HISTORIES

Adding variability of the phase angles to the input motion is a convenient approach for reaching a desired spatial coherency of the input motions, but there is an assumption of stationarity of the amplitude spectrum. As the more variability is added to the phase angles at higher frequencies to match the target coherency, this assumption of stationarity leads to time series that appear as constant amplitude for the full record. As a result, the non-stationary characteristics of the reference ground motion can be lost. An example of this is shown in Figure 7. The top trace shows the reference time history and the middle trace shows the modified time history with added phase variability located 500 m from the reference station. The two traces have the same Fourier amplitude spectra, but with the added phase variability the middle trace has spread out the energy over the complete time window.

To maintain the overall non-stationary characteristic of the reference time history and still match the target coherency function, the variability to the phase angles is added to short windows rather than using the complete time window. The recommended frequency-dependent time windows are listed in Table 1. For high frequencies, a short window length of 1.28 sec is used. The lengths are selected so that the number of points in the window is a power of 2 for use with a fast Fourier Transform without the need for padding. The phase variability for each time window is independent of the other time windows. An example of the time history using these time windows for adding the phase variability is shown by the lower trace in Figure 7. With this approach, the general non-stationarity of the reference time history is maintained.

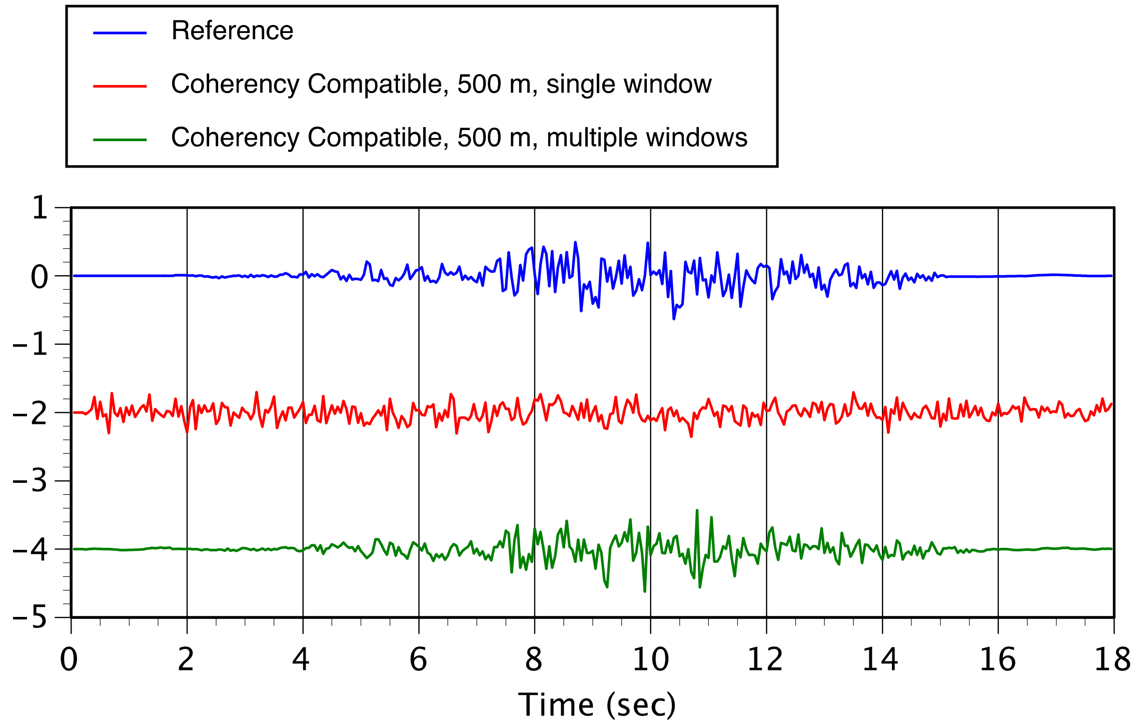

Figure 7. Example of the need for using frequency dependent window lengths when adding phase variability to the input motions. The top trace is the reference accelerogram. The middle and bottom traces show the accelerogram at a distance of 500 m from the reference trace using two different methods. The middle trace uses a single window length of the full record, whereas the bottom trace using the frequency dependent window lengths listed in Table 1.

Table 1: Time window length used for different frequencies.

Frequency Range (Hz)	Window Length (sec)
3 - 50	1.28
1 - 3	2.56
0.5 - 1	5.12
0.25 - 0.5	10.24
0.12 - 0.25	20.48
0.01 - 0.12	100

CONCLUSIONS

Using standard approaches for modelling the vertical ground motion component for SSI analysis, such as vertically propagating P waves, leads to overly coherent vertical ground motions that are likely part of the cause for the large vertical loads found in some SSI applications. Using more physically appropriate input motions and velocity models such as inclined P-SV waves in a stochastic medium leads to more realistic complexity of the vertical motions as measured by the spatial coherency, but it is not enough. Additional complexity is needed in the input motions.

The additional complexity can be added to the input motion using the variability of the phase angles. The standard deviation of the phase of the cross spectrum (phase differences between two stations) is closely related to the coherency. An advantage of using the standard deviation of the phase differences is that it is easy to partition the variability to the physical model with inclined P-SV waves in a stochastic medium and the input motions into the reduced SSI analysis domain.

Using the frequency-dependent time windows for adding the phase differences maintains the non-stationary characteristics of the input motion while adding the additional complexity to the input motions that is needed to match the empirical spatial coherency (combined effect of the physical model with inclined P-SV waves in a stochastic medium and the added complexity in the input motions).

The next steps are to (1) validate this approach comparing frequency-wavenumber spectrum from the generated motions with frequency-wavenumber spectra from 3-D dense arrays with earthquake recordings, and (2) compare the resulting vertical-component floor spectrum using the proposed approach and using the standard approach of modelling the vertical component as vertically propagating P waves.

REFERENCES

Bielak J, Loukakis K, Hisada Y, and Yoshimura C (2001). Domain reduction method for three–dimensional earthquake modeling in localized regions. part I: Theory. *Bulletin of the Seismological Society of America*, 93(2):817–824, 2003.

EPRI (2007). *Effects of Spatial Incoherence on Seismic Ground Motions. Technical report*, EPRI, Palo Alto, CA, 1015110, 2007.

Jeremic B, Jie G, Cheng Z, Tafazzoli N, Tasiopoulou P, Pisano F, Abell JA, Watanabe K, Feng Y, Sinha SK, Behbehani F, Yang H, and Wang H (1988-2021). *The Real-ESSI Simulator System*. University of California, Davis, 1988-2021. http://real-essi.us/.

Petersson, N. A., and B. Sjogreen (2015). Wave propagation in aniso- tropic elastic materials and curvilinear coordinates using a sum- mation-by-parts finite difference method, *J. Comp. Phys.* 299, 820–841, doi: 10.1016/j.jcp.2015.07.023.

Petersson, N. A., and B. E. Sjogreen (2018). SW4 Users Guide, Version 2.01, *Lawrence Livermore National Laboratory, LLNL-SM–741439*.

Zerva A (2009). *Spatial variation of seismic ground motions: modeling and engineering applications*. CRC Press, 2009. ISBN ISBN-10: 0849399297; ISBN-13: 978-0849399299.